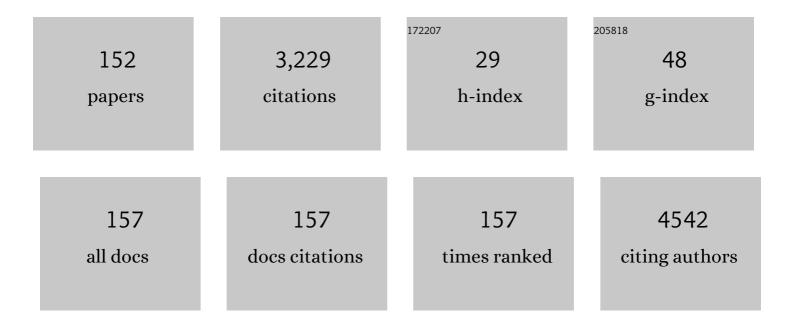
## Jakub Szlachetko

List of Publications by Year in descending order

Source: https://exaly.com/author-pdf/5997023/publications.pdf Version: 2024-02-01



LAKUR SZLACHETKO

#	Article	IF	CITATIONS
1	SwissFEL: The Swiss X-ray Free Electron Laser. Applied Sciences (Switzerland), 2017, 7, 720.	1.3	272
2	Catalytically Active and Spectator Ce <sup>3+</sup> in Ceriaâ€Supported Metal Catalysts. Angewandte Chemie - International Edition, 2015, 54, 8728-8731.	7.2	168
3	A von Hamos x-ray spectrometer based on a segmented-type diffraction crystal for single-shot x-ray emission spectroscopy and time-resolved resonant inelastic x-ray scattering studies. Review of Scientific Instruments, 2012, 83, 103105.	0.6	158
4	Polyhedral CeO <sub>2</sub> Nanoparticles: Size-Dependent Geometrical and Electronic Structure. Journal of Physical Chemistry C, 2012, 116, 7312-7317.	1.5	108
5	Revealing hole trapping in zinc oxide nanoparticles by time-resolved X-ray spectroscopy. Nature Communications, 2018, 9, 478.	5.8	84
6	Direct observation of charge separation on Au localized surface plasmons. Energy and Environmental Science, 2013, 6, 3584.	15.6	70
7	Physical Mechanisms and Scaling Laws of <mml:math xmlns:mml="http://www.w3.org/1998/Math/MathML" display="inline"&gt;<mml:mi>K</mml:mi>-Shell Double Photoionization. Physical Review Letters. 2009. 102. 073006.</mml:math 	2.9	68
8	Wavelength-dispersive spectrometer for X-ray microfluorescence analysis at the X-ray microscopy beamline ID21 (ESRF). Journal of Synchrotron Radiation, 2010, 17, 400-408.	1.0	64
9	Laboratory von Hámos X-ray spectroscopy for routine sample characterization. Review of Scientific Instruments, 2016, 87, 103105.	0.6	64
10	Synthesizing lead antimonate in ancient and modern opaque glass. Journal of Analytical Atomic Spectrometry, 2011, 26, 1040.	1.6	61
11	Scientific Opportunities for Heterogeneous Catalysis Research at the SuperXAS and SNBL Beam Lines. Chimia, 2012, 66, 699.	0.3	60
12	Tracking multiple components of a nuclear wavepacket in photoexcited Cu(I)-phenanthroline complex using ultrafast X-ray spectroscopy. Nature Communications, 2019, 10, 3606.	5.8	56
13	High energy resolution off-resonant spectroscopy at sub-second time resolution: (Pt(acac)2) decomposition. Chemical Communications, 2012, 48, 10898.	2.2	48
14	Au <sup>I</sup> Catalysis on a Coordination Polymer: A Solid Porous Ligand with Free Phosphine Sites. ChemCatChem, 2013, 5, 692-696.	1.8	43
15	Subsecond and in Situ Chemical Speciation of Pt/Al <sub>2</sub> O <sub>3</sub> during Oxidation–Reduction Cycles Monitored by High-Energy Resolution Off-Resonant X-ray Spectroscopy. Journal of the American Chemical Society, 2013, 135, 19071-19074.	6.6	43
16	Establishing nonlinearity thresholds with ultraintense X-ray pulses. Scientific Reports, 2016, 6, 33292.	1.6	43
17	A laboratory-based double X-ray spectrometer for simultaneous X-ray emission and X-ray absorption studies. Journal of Analytical Atomic Spectrometry, 2019, 34, 1409-1415.	1.6	40
18	High Energy Resolution Off-Resonant Spectroscopy for X-Ray Absorption Spectra Free of Self-Absorption Effects. Physical Review Letters, 2014, 112, 173003.	2.9	37

#	Article	IF	CITATIONS
19	Hydrogen evolution with nanoengineered ZnO interfaces decorated using a beetroot extract and a hydrogenase mimic. Sustainable Energy and Fuels, 2017, 1, 69-73.	2.5	35
20	Electronic and Geometric Structure of Ce <sup>3+</sup> Forming Under Reducing Conditions in Shaped Ceria Nanoparticles Promoted by Platinum. Journal of Physical Chemistry C, 2014, 118, 1974-1982.	1.5	34
21	E-beam evaporated TiO 2 and Cu-TiO 2 on glass: Performance in the discoloration of methylene blue and 2-propanol oxidation. Applied Catalysis A: General, 2016, 526, 191-199.	2.2	34
22	Structure of the methanol synthesis catalyst determined by in situHERFD XAS and EXAFS. Catalysis Science and Technology, 2012, 2, 373-378.	2.1	33
23	Separation of Two-Electron Photoexcited Atomic Processes near the Inner-Shell Threshold. Physical Review Letters, 2009, 102, 143001.	2.9	32
24	The oxidation state of copper in bimetallic (Pt–Cu, Pd–Cu) catalysts during water denitration. Catalysis Science and Technology, 2012, 2, 794.	2.1	32
25	Deconvolution of the Mechanism of Homogeneous Gold-Catalyzed Reactions. Organometallics, 2012, 31, 2395-2402.	1.1	31
26	Communication: The electronic structure of matter probed with a single femtosecond hard x-ray pulse. Structural Dynamics, 2014, 1, 021101.	0.9	31
27	Photopolymerized Polypyrrole Microvessels. Chemistry - A European Journal, 2012, 18, 310-320.	1.7	30
28	Real Time Determination of the Electronic Structure of Unstable Reaction Intermediates during Au <sub>2</sub> O <sub>3</sub> Reduction. Journal of Physical Chemistry Letters, 2014, 5, 80-84.	2.1	30
29	High-Resolution Study of X-Ray Resonant Raman Scattering at theKEdge of Silicon. Physical Review Letters, 2006, 97, 073001.	2.9	29
30	HERFD XAS/ATR-FTIR batch reactor cell. Physical Chemistry Chemical Physics, 2012, 14, 2164-2170.	1.3	29
31	In situ hard X-ray quick RIXS to probe dynamic changes in the electronic structure of functional materials. Journal of Electron Spectroscopy and Related Phenomena, 2013, 188, 161-165.	0.8	29
32	Temperature-programmed reduction of NiO nanoparticles followed by time-resolved RIXS. Physical Chemistry Chemical Physics, 2014, 16, 7692.	1.3	29
33	Chemical effects in the KÎ <sup>2</sup> X-ray emission spectra of sulfur. Nuclear Instruments & Methods in Physics Research B, 2007, 260, 642-646.	0.6	28
34	Evaluation of Pt and Re oxidation state in a pressurized reactor: difference in reduction between gas and liquid phase. Chemical Communications, 2011, 47, 6590.	2.2	27
35	First Observation of Two-Electron One-Photon Transitions in Single-Photon <mml:math xmlns:mml="http://www.w3.org/1998/Math/MathML" display="inline"&gt;<mml:mi>K</mml:mi>-Shell Double Ionization. Physical Review Letters, 2011_107_053001</mml:math 	2.9	27
36	Rational design of oxynitride materials: From theory to experiment. CrystEngComm, 2013, 15, 2583.	1.3	27

#	Article	IF	CITATIONS
37	High-resolution Laue-type DuMond curved crystal spectrometer. Review of Scientific Instruments, 2013, 84, 093104.	0.6	27
38	Spin cascade and doming in ferric hemes: Femtosecond X-ray absorption and X-ray emission studies. Proceedings of the National Academy of Sciences of the United States of America, 2020, 117, 21914-21920.	3.3	27
39	Relative detection efficiency of back- and front-illuminated charge-coupled device cameras for x-rays between 1keV and 18keV. Review of Scientific Instruments, 2007, 78, 093102.	0.6	26
40	Magnetic manipulation of molecules on a non-magnetic catalytic surface. Nanoscale, 2013, 5, 8462.	2.8	26
41	Determination of conduction and valence band electronic structure of anatase and rutile TiO 2. Journal of Chemical Sciences, 2014, 126, 511-515.	0.7	26
42	Application of the high-resolution grazing-emission x-ray fluorescence method for impurities control in semiconductor nanotechnology. Journal of Applied Physics, 2009, 105, 086101.	1.1	25
43	N-TiO2/Cu-TiO2 double-layer films: Impact of stacking order on photocatalytic properties. Journal of Catalysis, 2017, 353, 116-122.	3.1	25
44	High energy resolution fluorescence detection XANES – an in situ method to study the interaction of adsorbed molecules with metal catalysts in the liquid phase. Catalysis Science and Technology, 2013, 3, 1497.	2.1	24
45	Taking a snapshot of the triplet excited state of an OLED organometallic luminophore using X-rays. Nature Communications, 2020, 11, 2131.	5.8	24
46	High-resolution study of the x-ray resonant Raman scattering process around the1sabsorption edge for aluminium, silicon, and their oxides. Physical Review A, 2007, 75, .	1.0	23
47	Core-level nonlinear spectroscopy triggered by stochastic X-ray pulses. Nature Communications, 2019, 10, 4761.	5.8	23
48	Coupling a wavelength dispersive spectrometer with a synchrotron-based X-ray microscope: A winning combination for micro-X-ray fluorescence and micro-XANES analyses of complex artistic materials. Journal of Analytical Atomic Spectrometry, 2011, 26, 1051.	1.6	22
49	X-ray spectroscopic methods in the studies of nonstoichiometric TiO2â^'x thin films. Applied Surface Science, 2013, 281, 100-104.	3.1	22
50	Chemical State Analysis of Phosphorus Performed by X-ray Emission Spectroscopy. Analytical Chemistry, 2015, 87, 5632-5639.	3.2	22
51	Observation of ultralow-level Al impurities on a silicon surface by high-resolution grazing emission x-ray fluorescence excited by synchrotron radiation. Physical Review B, 2009, 80, .	1.1	21
52	Double <mml:math <br="" xmlns:mml="http://www.w3.org/1998/Math/MathML">display="inline"&gt;<mml:mrow><mml:mi>K</mml:mi></mml:mrow></mml:math> -shell photoionization and hypersatellite x-ray transitions of <mml:math <br="" xmlns:mml="http://www.w3.org/1998/Math/MathML">display="inline"&gt;<mml:mrow><mml:mn>12</mml:mn><mml:mo>⩽</mml:mo><mml:mi>Z</mml:mi><mml: Physical Review A, 2010, 82, .</mml: </mml:mrow></mml:math>	1.0 mo>⩽	21 <1
53	Hard x-ray absorption spectroscopy for pulsed sources. Physical Review B, 2013, 87, .	1.1	21
54	Direct Determination of Metal Complexes' Interaction with DNA by Atomic Telemetry and Multiscale Molecular Dynamics. Journal of Physical Chemistry Letters, 2017, 8, 805-811.	2.1	21

#	Article	IF	CITATIONS
55	Inelastic x-ray scattering in the vicinity of xenonL3edge. Physical Review A, 2007, 76, .	1.0	20
56	Depth-Resolved X-ray Absorption Spectroscopy by Means of Grazing Emission X-ray Fluorescence. Analytical Chemistry, 2015, 87, 10815-10821.	3.2	20
57	Transient mid-IR study of electron dynamics in TiO2 conduction band. Analyst, The, 2013, 138, 1966.	1.7	19
58	Determination of Conduction and Valence Band Electronic Structure of LaTiO x N y Thin Film. ChemSusChem, 2017, 10, 2099-2106.	3.6	19
59	A novel single-site manganese(ii) complex of a pyridine derivative as a catalase mimetic for disproportionation of H2O2 in water. Dalton Transactions, 2013, 42, 7761.	1.6	18
60	Scanning-free grazing emission x-ray fluorescence by means of an angular dispersive arrangement with a two-dimensional position-sensitive area detector. Review of Scientific Instruments, 2013, 84, 123102.	0.6	18
61	Novel in situ methodology to observe the interactions of chemotherapeutical Pt drugs with DNA under physiological conditions. Dalton Transactions, 2014, 43, 13839-13844.	1.6	18
62	Hydrated Electron Generation by Excitation of Copper Localized Surface Plasmon Resonance. Journal of Physical Chemistry Letters, 2019, 10, 1743-1749.	2.1	18
63	Calcareous sponge biomineralization: Ultrastructural and compositional heterogeneity of spicules in Leuconia johnstoni. Journal of Structural Biology, 2011, 173, 99-109.	1.3	17
64	Grazing angle X-ray fluorescence from periodic structures on silicon and silica surfaces. Spectrochimica Acta, Part B: Atomic Spectroscopy, 2014, 98, 65-75.	1.5	17
65	Depth profiling of dopants implanted in Si using the synchrotron radiation based highâ€resolution grazing emission technique. X-Ray Spectrometry, 2012, 41, 98-104.	0.9	16
66	High-energy-resolution grazing emission X-ray fluorescence applied to the characterization of thin Al films on Si. Spectrochimica Acta, Part B: Atomic Spectroscopy, 2013, 88, 136-149.	1.5	16
67	Effective catalytic disproportionation of aqueous H <sub>2</sub> O <sub>2</sub> with di- and mono-nuclear manganese( <scp>ii</scp> ) complexes containing pyridine alcohol ligands. Dalton Transactions, 2014, 43, 8599-8608.	1.6	16
68	Importance of the electronic structure of modified TiO 2 in the photoelectrochemical processes of hydrogen generation. International Journal of Hydrogen Energy, 2015, 40, 815-824.	3.8	16
69	Investigating DNA Radiation Damage Using X-Ray Absorption Spectroscopy. Biophysical Journal, 2016, 110, 1304-1311.	0.2	16
70	DoubleK-shell ionization of Al induced by photon and electron impact. Physical Review A, 2009, 79, .	1.0	15
71	Nanoparticle characterization by means of scanning free grazing emission X-ray fluorescence. Nanoscale, 2015, 7, 9320-9330.	2.8	15
72	Nonlinear XUV-optical transient grating spectroscopy at the Si L2,3–edge. Applied Physics Letters, 2019, 114, 181101.	1.5	15

#	Article	IF	CITATIONS
73	Mechanistic Insights into Oxygen Dynamics in Soot Combustion over Cryptomelane Catalysts in Tight and Loose Contact Modes via <sup>18</sup> O <sub>2</sub> / <sup>16</sup> O <sub>2</sub> Isotopic Variable Composition Measurements – A Hot Ring Model of the Catalyst Operation. ACS Catalysis, 2021, 11. 9530-9546.	5.5	15
74	Depth profiles of Al impurities implanted in Si wafers determined by means of the high-resolution grazing emission X-ray fluorescence technique. Spectrochimica Acta, Part B: Atomic Spectroscopy, 2010, 65, 445-449.	1.5	14
75	On the sensitivity of hard X-ray spectroscopies to the chemical state of Br. Physical Chemistry Chemical Physics, 2013, 15, 11088.	1.3	13
76	Tracking the Temporal Dynamics of Intracellular Lead Speciation in a Green Alga. Environmental Science & Technology, 2015, 49, 11176-11181.	4.6	13
77	Application of wavelength dispersive Xâ€ray spectroscopy to improve detection limits in Xâ€ray analysis. X-Ray Spectrometry, 2011, 40, 2-6.	0.9	12
78	Fine tuning of gold electronic structure by IRMOF post-synthetic modification. RSC Advances, 2013, 3, 12043.	1.7	12
79	Geometrical optics modelling of grazing incidence X-ray fluorescence of nanoscaled objects. Journal of Analytical Atomic Spectrometry, 2013, 28, 689.	1.6	12
80	An operando emission spectroscopy study of Pt/Al <sub>2</sub> O <sub>3</sub> and Pt/CeO <sub>2</sub> /Al <sub>2</sub> O <sub>3</sub> . Physical Chemistry Chemical Physics, 2016, 18, 29268-29277.	1.3	12
81	A Dispersive Inelastic X-ray Scattering Spectrometer for Use at X-ray Free Electron Lasers. Applied Sciences (Switzerland), 2017, 7, 899.	1.3	12
82	X-ray emission spectroscopy: highly sensitive techniques for time-resolved probing of cerium reactivity under catalytic conditions. Physical Chemistry Chemical Physics, 2016, 18, 32486-32493.	1.3	11
83	Hidden gapless states during thermal transformations of preorganized zinc alkoxides to zinc oxide nanocrystals. Materials Horizons, 2018, 5, 905-911.	6.4	11
84	Soot Combustion over Niobium-Doped Cryptomelane (K-OMS-2) Nanorods—Redox State of Manganese and the Lattice Strain Control the Catalysts Performance. Catalysts, 2020, 10, 1390.	1.6	11
85	High energy resolution off-resonant spectroscopy: A review. Spectrochimica Acta, Part B: Atomic Spectroscopy, 2017, 136, 23-33.	1.5	10
86	A von Hamos spectrometer for <i>in situ</i> sulfur speciation by non-resonant sulfur Kα emission spectroscopy. Journal of Analytical Atomic Spectrometry, 2019, 34, 2105-2111.	1.6	10
87	Determination of conduction and valence band electronic structure of La2Ti2O7 thin film. RSC Advances, 2014, 4, 11420.	1.7	9
88	Differences between bulk and surface electronic structure of doped TiO2 with soft-elements (C, N and) Tj ETQc	10 0 0 rgBT 2.0	Oyerlock 10

89	The influence of nitrogen doping on the electronic structure of the valence and conduction band in TiO <sub>2</sub> . Journal of Synchrotron Radiation, 2019, 26, 145-151.	1.0	9
90	X-ray absorption and emission spectroscopy of TiO2 thin films with modified anionic sublattice. Radiation Physics and Chemistry, 2013, 93, 40-46.	1.4	8

#	Article	IF	CITATIONS
91	Heterogenized Gold(I)–Carbene as a Single‣ite Catalyst in Continuous Flow. ChemCatChem, 2014, 6, 443-448.	1.8	8
92	Optical design of the ARAMIS-beamlines at SwissFEL. AIP Conference Proceedings, 2016, , .	0.3	8
93	Cr-doping effects on unoccupied d-band electronic structure of TiO2. Chemical Physics Letters, 2016, 664, 73-76.	1.2	8
94	<i>Onâ€ŧheâ€fly</i> Catalyst Accretion and Screening in Chemoselective Flow Hydrogenation. ChemCatChem, 2018, 10, 3641-3646.	1.8	8
95	The enhancement effect in K-shell radiative recombination of \$mbox{sffamilyfseries U}^{hbox{sffamilyfseriesontsize{10}{12}selectfont 92+}}\$ ions with cooling electrons. European Physical Journal: Special Topics, 2009, 169, 15-18.	1.2	7
96	L-subshell Coster-Kronig yields of palladium determined via synchrotron-radiation-based high-resolution x-ray spectroscopy. Physical Review A, 2009, 80, .	1.0	7
97	Subshell-selective x-ray studies of radiative recombination of <mml:math xmlns:mml="http://www.w3.org/1998/Math/MathML"&gt; <mml:msup> <mml:mrow> <mml:mi mathvariant="normal"&gt;U </mml:mi </mml:mrow> <mml:mrow> <mml:mn>92 </mml:mn> <mml:mo> + </mml:mo> with electrons for very low relative energies. Physical Review A, 2015, 92, .</mml:mrow></mml:msup></mml:math 	> < /mml:mr	row?
98	Insights into the structure–activity relationships of chiral 1,2-diaminophenylalkane platinum(II) anticancer derivatives. Journal of Biological Inorganic Chemistry, 2015, 20, 841-853.	1.1	7
99	Mechanism of hydrolysis of a platinum(IV) complex discovered by atomic telemetry. Journal of Inorganic Biochemistry, 2018, 187, 56-61.	1.5	7
100	Inception of electronic damage of matter by photon-driven post-ionization mechanisms. Structural Dynamics, 2019, 6, 024901.	0.9	7
101	Comparative study of the around-Fermi electronic structure of 5 <i>d</i> metals and metal-oxides by means of high-resolution X-ray emission and absorption spectroscopies. Journal of Synchrotron Radiation, 2020, 27, 689-694.	1.0	7
102	Heterogeneous Catalysis Experiments at XFELs. Are we Close to Producing a Catalysis Movie?. Catalysis Letters, 2014, 144, 197-203.	1.4	6
103	Incorporation of chromium into TiO2 nanopowders. Materials Research Bulletin, 2015, 64, 112-116.	2.7	6
104	Resonant X-ray emission spectroscopy of platinum( <scp>ii</scp> ) anticancer complexes. Analyst, The, 2016, 141, 1226-1232.	1.7	6
105	A compact and versatile tender X-ray single-shot spectrometer for online XFEL diagnostics. Journal of Synchrotron Radiation, 2018, 25, 16-19.	1.0	6
106	Resonant X-ray Raman scattering for Al, Si and their oxides. Nuclear Instruments & Methods in Physics Research B, 2005, 238, 353-356.	0.6	5
107	A 2D position sensitive germanium detector for spectroscopy and polarimetry of high-energetic x-rays. Journal of Physics: Conference Series, 2007, 58, 411-414.	0.3	5
108	A DuMond-type crystal spectrometer for synchrotron-based X-ray emission studies in the energy range of 15–26 keV. Review of Scientific Instruments, 2019, 90, 063106.	0.6	5

#	Article	IF	CITATIONS
109	Determination of Crystal-Field Splitting Induced by Thermal Oxidation of Titanium. Journal of Physical Chemistry A, 2021, 125, 50-56.	1.1	5
110	Reduction Mechanisms of Anticancer Osmium(VI) Complexes Revealed by Atomic Telemetry and Theoretical Calculations. Inorganic Chemistry, 2021, 60, 6663-6671.	1.9	5
111	Properties of polycapillary optics dedicated to low-energy parallel-beam wavelength-dispersive spectrometers for synchrotron-based X-ray fluorescence study. Optics Express, 2021, 29, 27193.	1.7	5
112	Implementation of a crossed-slit system for fast alignment of sealed polycapillary X-ray optics. Journal of Synchrotron Radiation, 2020, 27, 1730-1733.	1.0	5
113	High-resolutionKMMradiative Auger x-ray emission spectra of calcium induced by synchrotron radiation. Physical Review A, 2011, 83, .	1.0	4
114	Determination of catalytic reaction mechanisms by isotopic frequency response. Analyst, The, 2012, 137, 5374.	1.7	4
115	X-ray two-photon absorption with high fluence XFEL pulses. Journal of Physics: Conference Series, 2015, 635, 102009.	0.3	4
116	Study of the reactivity of silica supported tantalum catalysts with oxygen followed by in situ HEROS. Physical Chemistry Chemical Physics, 2015, 17, 18262-18264.	1.3	4
117	Electronic structure of Fe, α-Fe 2 O 3 and Fe(NO 3 ) 3 × 9 H 2 O determined using RXES. Chemical Physics, 2017, 493, 49-55.	0.9	4
118	Boosting the Performance of Nano-Ni Catalysts by Palladium Doping in Flow Hydrogenation of Sulcatone. Catalysts, 2020, 10, 1267.	1.6	4
119	Operation of a bending magnet beamline in large energy bandwidth mode for non-resonant X-ray emission spectroscopy. Results in Physics, 2020, 18, 103212.	2.0	4
120	Fluorescence X-ray micro-spectroscopy activities at ESRF. Journal of Physics: Conference Series, 2009, 186, 012014.	0.3	3
121	Synchrotron radiation based micro X-ray fluorescence analysis of the calibration samples used in surface sensitive total reflection and grazing emission X-ray fluorescence techniques. Radiation Physics and Chemistry, 2013, 93, 117-122.	1.4	3
122	Controlling dark catalysis with quasi half-cycle terahertz pulses. Catalysis Science and Technology, 2017, 7, 1050-1054.	2.1	3
123	State-Population Narrowing Effect in Two-Photon Absorption for Intense Hard X-ray Pulses. Applied Sciences (Switzerland), 2017, 7, 653.	1.3	3
124	Cross-section determination for one- and two-photon absorption of cobalt at hard-x-ray energies. Physical Review A, 2019, 99, .	1.0	3
125	Operando sulfur speciation during sulfur poisoning-regeneration of Ru/SiO2 and Ru/Al2O3 using non-resonant sulfur Kî±1,2 emission. RSC Advances, 2020, 10, 15853-15859.	1.7	3
126	Low-Angle X-Ray Spectroscopy and Reflectometry Techniques in Interdisciplinary Applications. Acta Physica Polonica A, 2021, 139, 247-256.	0.2	3

Jakub Szlachetko

#	Article	IF	CITATIONS
127	Microliter-stirred sample setup for X-ray spectroscopy analysis of nanomaterials in suspension. Spectrochimica Acta, Part B: Atomic Spectroscopy, 2022, 189, 106367.	1.5	3
128	Techniques: RXES, HR-ÂXAS, HEROS, GIXRF, and GEXRF. , 2014, , 59-116.		2
129	The use of Resonant X-ray Emission Spectroscopy (RXES) for the electronic analysis of metal complexes and their interactions with biomolecules. Drug Discovery Today: Technologies, 2015, 16, 1-6.	4.0	2
130	<i>In situ</i> observation of charge transfer and crystal field formation <i>via</i> high energy resolution X-ray spectroscopy during temperature programmed oxidation. Physical Chemistry Chemical Physics, 2020, 22, 14731-14735.	1.3	2
131	Femtosecond X-ray spectroscopy of haem proteins. Faraday Discussions, 2021, 228, 312-328.	1.6	2
132	Olefin Hydrogenation with Single-Site Gold. Acta Physica Polonica A, 2014, 125, 940-943.	0.2	2
133	Approaching the Attosecond Frontier of Dynamics in Matter with the Concept of X-ray Chronoscopy. Applied Sciences (Switzerland), 2022, 12, 1721.	1.3	2
134	STATE-SELECTIVE X-RAY STUDY OF THE RADIATIVE RECOMBINATION OF U92+ IONS WITH COOLING ELECTRONS. , 2006, , .		1
135	Double K-shell photoionization of low-Z atoms and He-like ions. European Physical Journal: Special Topics, 2009, 169, 23-27.	1.2	1
136	Observation of enhancement in K-shell radiative recombination of U <sup>92+</sup> ions with cooling electrons. Journal of Physics: Conference Series, 2009, 194, 062017.	0.3	1
137	Single-photon double K-shell ionization of low-Z atoms. Journal of Physics: Conference Series, 2010, 212, 012006.	0.3	1
138	Hydrodechlorination Using Pd–Au Nanoparticles to Convert Chloro-Containing Compounds to Useful Chemicals. , 2016, , .		1
139	In situ high energy resolution off-resonant spectroscopy applied to a time-resolved study of single site Ta catalyst during oxidation. Nuclear Instruments & Methods in Physics Research B, 2017, 411, 63-67.	0.6	1
140	Preliminary results of human PrP C protein studied by spectroscopic techniques. Nuclear Instruments & Methods in Physics Research B, 2017, 411, 121-128.	0.6	1
141	Xâ€Ray Spectroscopy on Biological Systems. , 0, , .		1
142	Resonant X-ray Emission Spectroscopy with a SASE Beam. Applied Sciences (Switzerland), 2021, 11, 8775.	1.3	1
143	Double K-shell photoionization and universal scaling laws. Journal of Physics: Conference Series, 2009, 194, 022040.	0.3	0
144	Enhanced radiative recombination of U92+ions with cooling electrons for the K-shell. Journal of Physics: Conference Series, 2012, 388, 062044.	0.3	0

#	Article	IF	CITATIONS
145	Time-resolved X-ray absorption and emission spectroscopy on ZnO nanoparticles in solution. , 2014, , .		Ο
146	Two-photon absorption using off-resonant excitation with ultrashort X-ray pulses. Journal of Physics: Conference Series, 2015, 635, 092147.	0.3	0
147	Novel reference-free methods for the determination of the instrumental response of Laue-type bent crystal spectrometers. Journal of Analytical Atomic Spectrometry, 2019, 34, 2325-2332.	1.6	Ο
148	Enhanced polarization transfer to the characteristic Lα x-ray lines near the nonlinear Cooper minimum of two-photon ionization. Physical Review A, 2020, 102, .	1.0	0
149	Pulsed laser-plasma soft X-ray source as a compact tool for X-ray absorption spectroscopy of metal oxides. Journal of Instrumentation, 2020, 15, C05026-C05026.	0.5	Ο
150	Femtosecond X-ray Absorption and Emission Spectroscopy on ZnO Nanoparticles in Solution. , 2016, , .		0
151	Synchrotron and X-Ray Free Electron Laser Studies of High-Valent Iron Formation with X-ray Absorption Spectroscopy. , 2016, , .		Ο
152	Femtosecond Molecular Flattening in [Cu(dmp)2]+ Probed by X-ray Emission Spectroscopy and Solution Scattering. , 2020, , .		0